

Settlement behaviour of a pile raft subjected to vertical loadings in multilayered soil

Raj Banerjee, Srijit Bandyopadhyay, Aniruddha Sengupta & G. R. Reddy

To cite this article: Raj Banerjee, Srijit Bandyopadhyay, Aniruddha Sengupta & G. R. Reddy (2020): Settlement behaviour of a pile raft subjected to vertical loadings in multilayered soil, Geomechanics and Geoengineering, DOI: [10.1080/17486025.2020.1739754](https://doi.org/10.1080/17486025.2020.1739754)

To link to this article: <https://doi.org/10.1080/17486025.2020.1739754>



Published online: 06 Apr 2020.



Submit your article to this journal [↗](#)



Article views: 48



View related articles [↗](#)



View Crossmark data [↗](#)



Settlement behaviour of a pile raft subjected to vertical loadings in multilayered soil

Raj Banerjee ^a, Srijit Bandyopadhyay^a, Aniruddha Sengupta^b and G. R. Reddy^a

^aStructural and Safety Engineering Section, Bhabha Atomic Research Centre, Mumbai, India; ^bCivil Engineering Department, Indian Institute of Technology, Kharagpur, India

ABSTRACT

The performances of a piled raft system in terms of serviceability and load-carrying capacity have been reviewed. The settlement behaviour of a square-piled raft in a layered soil is investigated using numerical analysis. The emphasis is given on quantifying the reduction of the average and the differential settlements of the raft in layered soil. A 3D finite element analysis using a commercial software called PLAXIS 3D (Version 2) is performed for various pile positions, pile numbers and pile lengths under the raft subjected to a uniform vertical loading. The settlement aspects for an efficient design of a piled raft subjected to vertical loadings have been addressed. It is found that the required piled group-raft area ratio (B_g/B_r) for minimising the differential settlement of a raft in a layered soil should be within a range of 0.4 to 0.6.

ARTICLE HISTORY

Received 31 October 2019
Accepted 26 February 2020

KEYWORDS

Raft foundation; embedded piles; piled raft foundation; differential settlement; PLAXIS 3D

1. Introduction

A pile foundation is being used in the civil engineering practice for many years to transmit the superstructure loads to a competent soil layer at a depth. The structures, like, high rise buildings, bridges, chimneys, nuclear power reactors and offshore jetties/rigs are generally subjected to heavy lateral loads due to wind forces, water forces, earthquake forces, etc. The shallow foundations are not good in carrying high lateral loads and under those circumstances a pile foundation is recommended. The pile foundations are also utilised when the soil immediately beneath a structure is weak and the superstructure loads need to be transmitted to a competent soil located at a depth. The most notable work on this topic is by Matlock (1970), Matlock and Reese (1960), Meyer and Reese (1979), Reese (1977), Reese and Junius (1977), Poulos (1971), and Broms (1964a, 1964b). The use of a piled raft foundation has become more popular in the recent years, as the combined action of the raft and the piles can increase the bearing capacity, reduce settlement, and the piles can be arranged to reduce the differential movement of the raft. A piled raft foundation is a geotechnical composite construction consisting of three elements – piles, raft and the subsoil. When a raft foundation alone does not satisfy the design requirements, as in the case of heavy structures, like, a nuclear reactor located in a marshy coastal area, it may be possible to enhance the performance of the raft by the addition of piles

underneath it. The use of a limited number of piles may improve the ultimate load capacity, the settlement and the differential settlement of a raft and reduce the required thickness of a raft (Poulos 2001). Balakumar *et al.* (2013) have outlined a simple analytical procedure and effectiveness of pressuremeter tests in predicting piled raft behaviour which can be utilised in the detailed design of such system. Katzenbach *et al.* (2005) have given an overview of the theoretical and the practical development of piled raft foundation and its use in the reduction of settlement in the high rise buildings. Butterfield and Banerjee (1971) have analysed pile-soil-cap interaction using Mindlin's equation and found the load sharing between the piles and the cap. According to them, the load sharing by a pile cap ranges from 20% to 60% depending upon the pile spacing. Poulos (1994) has presented an approximate numerical analysis of the pile-raft interaction. The raft is modelled as a thin plate and the piles as interacting springs. The settlements thus predicted are in agreement with the centrifuge tests and the full-scale tests on a piled raft. Nguyen *et al.* (2013) have performed a centrifuge test and Plaxis 3D analysis of a piled raft in sand and proposed a design method for a vertically loaded piled raft considering the interaction effects. Bourgeois *et al.* (2012) have also performed settlement analysis of a vertically loaded piled raft by means of a multiphase model accounting for soil-pile interaction. The literature survey shows that enormous

attention has been focussed on the development of analytical models for a piled raft (Clancy and Randolph (1993), Franke *et al.* (1994), Ta and Small (1996)). This development subsequently has resulted in numerous parametric studies that have investigated the influences of geometry and soil conditions on the performances of a piled raft. Laboratory and field tests on piled rafts and pile groups have been also conducted and have provided useful insights into the behaviours of piled rafts and pile groups (Horikoshi and Randolph (1998)). The case histories, in which extensive field measurements are made, have been also reported in the literature (Franke *et al.* (1994)). Ibrahim (2013) has used Plaxis 3D to evaluate the effect of piles in reducing the settlement and the contribution of a raft in increasing load-carrying capacity. Franke (1991) has demonstrated with the help of instrumentation of four buildings that a piled raft reduces the settlement by about 50% as compared to a raft alone. Lee *et al.* (2010) developed a three-dimensional model of a piled raft and suggested that the limited number of piles placed strategically under a raft may result in the improvement of both, the bearing capacity, and the settlement of a piled raft. Cho *et al.* (2012) have also studied settlement behaviours of a piled raft and their objective has been also to reduce the differential settlement and to find out the optimum pile group-raft area ratio (B_g/B_r) for clayey soil. EI-Garhy *et al.* (2013) have conducted experiments on model piled rafts in sandy soil to investigate the behaviour of a raft on settlement reducing piles. They have performed tests on model single pile, un-piled rafts and rafts on 1, 4, 9, or 16 piles. The results of the tests show the effectiveness of using piles as settlement reduction measure along with the rafts. As the number of settlement reducing piles increases, the load improvement ratio increases and the differential settlement reduces significantly. Elwakil and Azzam (2016) have performed small-scale model tests on piled raft in cohesionless soil. The effects of the pile length and the alignment on the attained ultimate load are experimentally investigated. From the study, it has been concluded that as the length of piles and the number of piles decrease, the load carried by raft increases. Park *et al.* (2016) have studied the load-carrying behaviour of driven piled rafts embedded in sand using the 3-D finite element analysis. Their work highlights that the load sharing ratios for driven piles are higher than those for bored piles within a certain range of settlement. With further increase in settlement, however, the values of load sharing ratio for driven piles became similar to those for bored piles with limited variation. Rabiei and Choobbasti (2016) have presented the design of

combined pile raft by placing the piles beneath the footing in an economic way. This study focuses on investigating the settlement behaviours of a heavy structure (thermal power plant) on piled raft in layered soil under vertical loading using 3D finite element analysis and the concept of embedded piles. Only a handful of studies has been conducted on piled raft resting on layered soil with an aim of finding out the optimum pile group-raft area ratio (B_g/B_r) for minimising the differential settlement of a raft. Hence, an attempt has been made in this paper to fill this grey area.

2. Measured and computed load responses of a vertically loaded piled raft

A 3D numerical model of a piled raft and the surrounding soils have been developed in the PLAXIS 3D (Brinkgreve and Swolfs (2007)) for the present study. The validation of the 3D finite element model is examined by comparing the results with those from the experiments conducted on dry cohesionless soil reported by Elwakil and Azzam (2016). Twenty three numbers of tests have been conducted to study the behaviours of a piled raft under vertical loading. Out of these, two tests are chosen for validation. The first test is performed on a 16 number of piles located under a 150 mm x 150 mm raft with 15 mm in thickness. Each pile is 400 mm in length and 12 mm in diameter. The second test is performed on a same-size raft without any pile. The piled raft is located at the middle of a soil domain of 750 mm diameter on plan and 600 mm in depth. The bottom boundary is considered fixed, that is, the horizontal and vertical movements are restrained. The side boundaries are assumed to be on roller, that is, movements in the horizontal directions are restrained. The subsoil comprises dry sand whose behaviour is represented by elastic-perfectly plastic Mohr-Coulomb model. The quadratic 15-noded wedge elements are utilised to model the subsoil. The properties of the subsoil as reported by Elwakil and Azzam (2016) and used in the present analysis are tabulated in Table 1. It is to be noted that although the dilation angle has been reported to be 5° by Elwakil and Azzam (2016) in their

Table 1. Soil properties used in the model validation.

Soil Parameter	Value
Poisson's ratio	0.3
Young's Modulus (MPa)	5.0
Angle of internal friction (ϕ')	35°
Dilation angle (ψ')	0°
Cohesion (c') (kPa)	1.0
Saturated unit weight, γ_{sat} (kN/m ³)	19.5
Dry unit weight, γ_{dry} (kN/m ³)	18.0

paper, in the present numerical analysis, it has been assumed to be zero, and a small amount of cohesion has been added to improve the numerical stability. The common practice is to take dilation angle equal to ϕ , where ' ϕ ' is the angle of internal friction of the soil (Plaxis 3D Version 2). In this paper, the dilation angle is assumed to be zero, as there is no horizontal (shear force) loading on the piled raft which will induce shear-induced volumetric settlement.

The piles are assumed to be made of steel with a circular cross-section of 12 mm in diameter. The piles are modelled by embedded pile element. The pile installation process is rather complicated and not modelled here. The stress change in the soil during the pile installation is therefore not included (wished in place) to model the bored piles. The piles are assumed to be in a stress-free state at the start of the analysis (following Jeong *et al.* (2004)). The raft is also made of steel and numerically modelled by plate elements. The raft is modelled as an isotropic elastic material with material parameters given by modulus of elasticity, $E = 21 \times 10^7$ kPa and Poisson's ratio, $\gamma = 0.25$. The pile heads are assumed to be connected to the raft rigidly. Figure 1(a–c) shows the model, which consist of the raft and the piled raft along with the location of piles underneath the raft, with proper boundary conditions. The load on top of the raft has been applied as a uniformly distributed load till the desired load limit of the experiment (= 62.2 kPa, which is equal to 1.40 kN for piled raft and 53.3 kPa, which is equal to 1.20 kN for the raft) is reached.

The embedded pile elements consider the piles as slender beam elements, which are connected to the surrounding soil by embedded skin interfaces and embedded foot interfaces which can penetrate the soil volume elements at any arbitrary location and orientation. Although the diameter d , the unit weight, γ and the modulus, E are assigned to the embedded beam element, it remains a line element in the finite element model. The diameter, d , in the material data set determines an elastic zone in the soil around the beam (pile) in order to avoid failure in a soil element which should physically be a pile element (Engin (2006)). During the post-mesh-generation stage, new nodes are generated representing the pile nodes at the intersection points between the pile and the soil elements (Sadek and Shahrour (2004)). The pile–soil interaction is represented by the skin friction (in kN/m) and the interaction at the base of the pile, known as foot resistance (in kN). For describing the behaviour of the interface, an elastic perfectly plastic failure criterion is used to distinguish between the interface at the skin friction and at the foot of the pile. The skin friction at the pile–soil interface is represented in axial and both horizontal directions by the relationships given in Equations (1)–(3):

$$T_{ay} = K_{ay} (\Delta_{ay}^{pile} - \Delta_{ay}^{soil}) \quad (1)$$

$$T_{nx} = K_{nx} (\Delta_{nx}^{pile} - \Delta_{nx}^{soil}) \quad (2)$$

$$T_{nz} = K_{nz} (\Delta_{nz}^{pile} - \Delta_{nz}^{soil}) \quad (3)$$

where T_{ay} , T_{nx} and T_{nz} are the skin frictions along the axial and the two horizontal (x and z) directions, respectively. K_{ay} , K_{nx} and K_{nz} are the stiffnesses in the axial and the two horizontal directions. Δ_{ay}^{pile} , Δ_{nx}^{pile} and Δ_{nz}^{pile} are the axial and the lateral deformations of a pile element. Δ_{ay}^{soil} , Δ_{nx}^{soil} and Δ_{nz}^{soil} are the axial and the lateral deformations of the soil domain. For the definition of the skin resistance, three different definitions are illustrated. The first and the simplest one is a linear distribution, where a constant or a linear distribution for the ultimate skin resistance is defined. The second option is the so-called multi-linear distribution, where it is possible to define different values for the skin friction at depths. This is, for example, necessary when layered soils are encountered and therefore different skin resistances are present along a pile. It is important to note that this definition implies that the bearing capacity of a pile is assumed beforehand and not a result of the analysis, as the maximum skin friction is predefined. The third way to define a skin resistance is the layer dependent option, where the interface behaviour is related to the strength parameters of the adjacent soil and the normal stresses along the interface. When using the layer dependent option, the embedded interface elements behave similar to normal interface elements as used for volume piles (Equation 4) and therefore the input for the layer dependent option is an R_{inter} value for the strength reduction. In addition, a limiting value for the skin resistance is defined.

$$\tau = R_{inter} c'_n + R_{inter} \sigma'_n \tan(\phi'_n) \quad (4)$$

where τ is the shear strength of the soil. c'_n and ϕ'_n are the effective cohesion and the effective angle of internal friction of the soil. σ'_n is the effective normal stress acting on the soil.

In this study, we have chosen the simplest option, which is the first one. A constant distribution of skin friction has been assumed whose value is found to be 0.07 kN/m. In addition to the skin resistance, the tip resistance is governed by a non-linear spring at the pile tip. It may be formulated as below:

$$F_{tip} = K_{tip} (\Delta_{tip}^{pile} - \Delta_{tip}^{soil}) \quad (5)$$

where F_{tip} is the tip resistance of the pile element, which depends upon the relative deformation of the soil and the pile. K_{tip} is the stiffness near the tip of the pile.

A maximum base resistance (F_{max}) is assigned to the non-linear spring elements at the base of an embedded pile

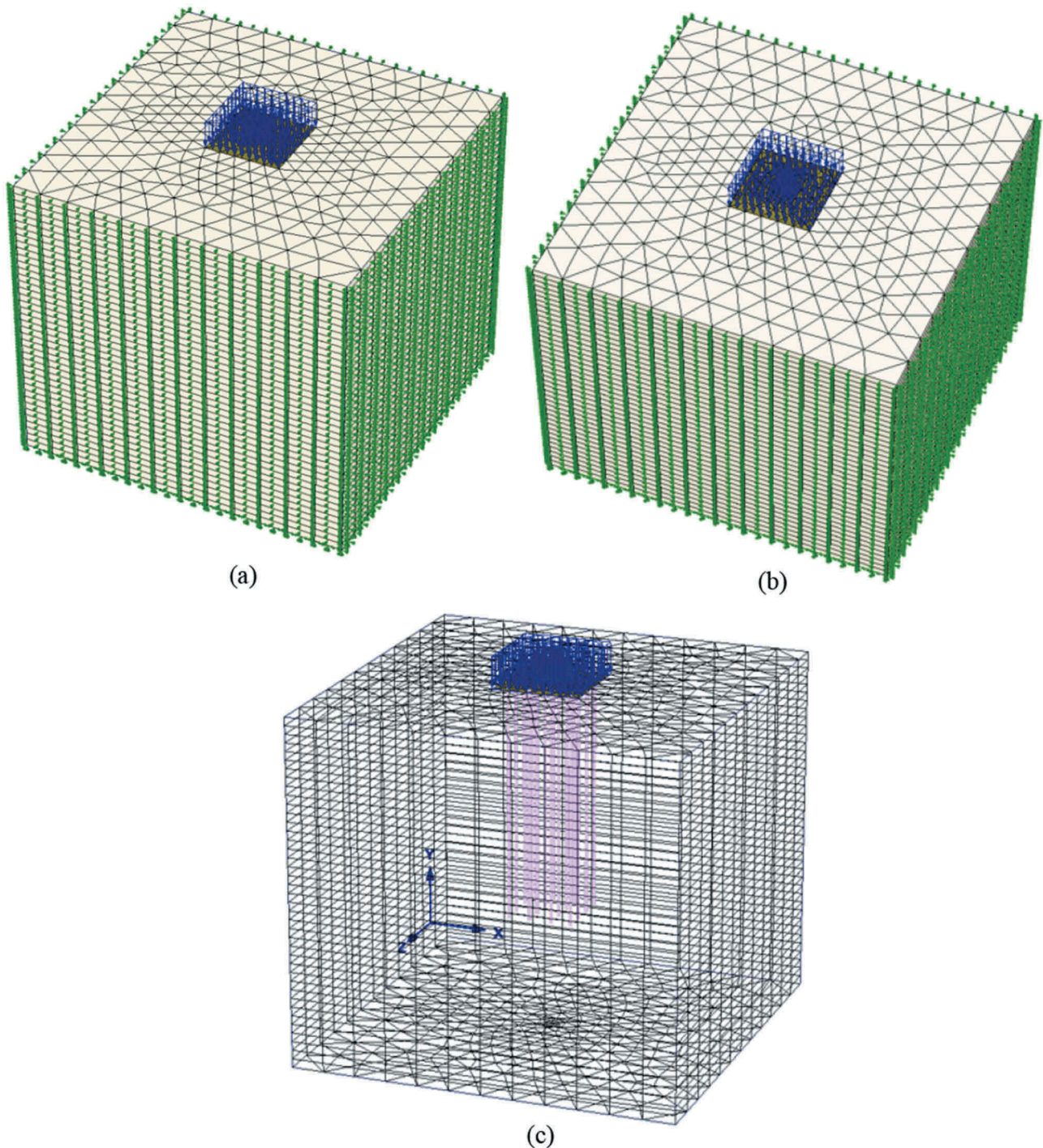


Figure 1. (a). A typical 3D finite element mesh of a raft and (b) a piled raft with soil domain (c) location of piles underneath the raft.

(= 0.3 kN, in this study). The value is chosen in such a way that the base resistance does not affect the numerical results. A drained analysis has been performed to study the long-term behaviour of the raft alone and the piled raft subjected to a uniform vertical loading corresponding to the applied loads during the tests reported by Elwakil and Azzam (2016). Figure 2(a,b) shows the comparison of the deformed mesh of the raft and the piled raft at the end of the loading.

It may be seen that the maximum deformation is 1.64 mm in the case of the piled raft and 4.03 mm in the case of the raft alone. Two piles at the two locations (at the corner and the centre) on the raft have been chosen to observe the values of skin friction mobilised in the piles. It is observed that the skin friction of all the piles has been completely mobilised, although the skin friction of two piles only is shown in Figure 3(a,b). The piles are driven piles in the

experiments done by Elwakil and Azzam (2016), hence the maximum resistance comes through the skin friction (as it is completely mobilised) which is also observed in this numerical study. In addition, the vertical stress contours of the piled raft are shown in Figure 4 by taking a vertical section from the middle of the piled raft along the y-axis.

Finally, the numerically obtained vertical load-displacements of the raft and the piled raft are compared with the experimental measurements reported by Elwakil and Azzam (2016) and shown in Figure 5. The vertical displacement is measured at the two ends of the raft, as seen from the experimental setup performed by Elwakil and Azzam (2016). Hence, in the numerical study, the average load-displacement responses at the two ends have been taken. It is observed that the experimental and the numerical results are varying within a tolerable limit, although the raft is giving a less stiffer response throughout the numerical analysis.

3. Numerical study of a large-piled raft in multilayered soil

After the successful validation of the numerical model, the behaviour of a piled raft (PR) with different pile lengths, pile spacing and configurations is investigated. The piles are made of solid (M 35 concrete) circular cross-section with 0.8 m in diameter (d) and, 15 m and 25 m (floating) in

length (L), modelled by embedded pile elements. The 18 m by 18 m raft with a thickness of 1.5 m is assumed to be also made of M 35 grade concrete and numerically modelled by a plate element. The raft is modelled as an isotropic, elastic material with material parameters given by $E = 29,580 \text{ MPa}$, $\gamma_{\text{raft}} = 24 \text{ kN/m}^3$. The pile heads are assumed to be connected to the raft rigidly. The quadratic 15-noded wedge elements are utilised to model the subsoil. The piled raft and the raft are resting on a multilayered soil (material properties are based on borehole logs) of a site in Punjab, India, where strategic buildings (on raft or piled raft) are to be constructed. Hence, the subsoil profile at Punjab is chosen for the settlement analysis. The material behaviour of the soil layers is modelled by Mohr-Coulomb model (drained strength). The soil parameters are given in Table 2. The raft and the piled raft are subjected to a vertical pressure of 500 kPa, which represents the equivalent vertical loading of a heavy industrial structure (thermal power plant). Figure 6(a,b) shows a typical 3D FE mesh along with the raft and the piles, used in this analysis. The horizontal extent and the vertical extent of the foundation soil domain are 80 m and 50 m, respectively. These dimensions are considered to be sufficient to keep the influence zone of the piled raft within the soil domain. In order to justify the soil dimensions to be free from the boundary effects, the vertical deformation and the stress contours are plotted in Figure 7(a,b) by taking a vertical section along the y-axis in a piled raft at the end of

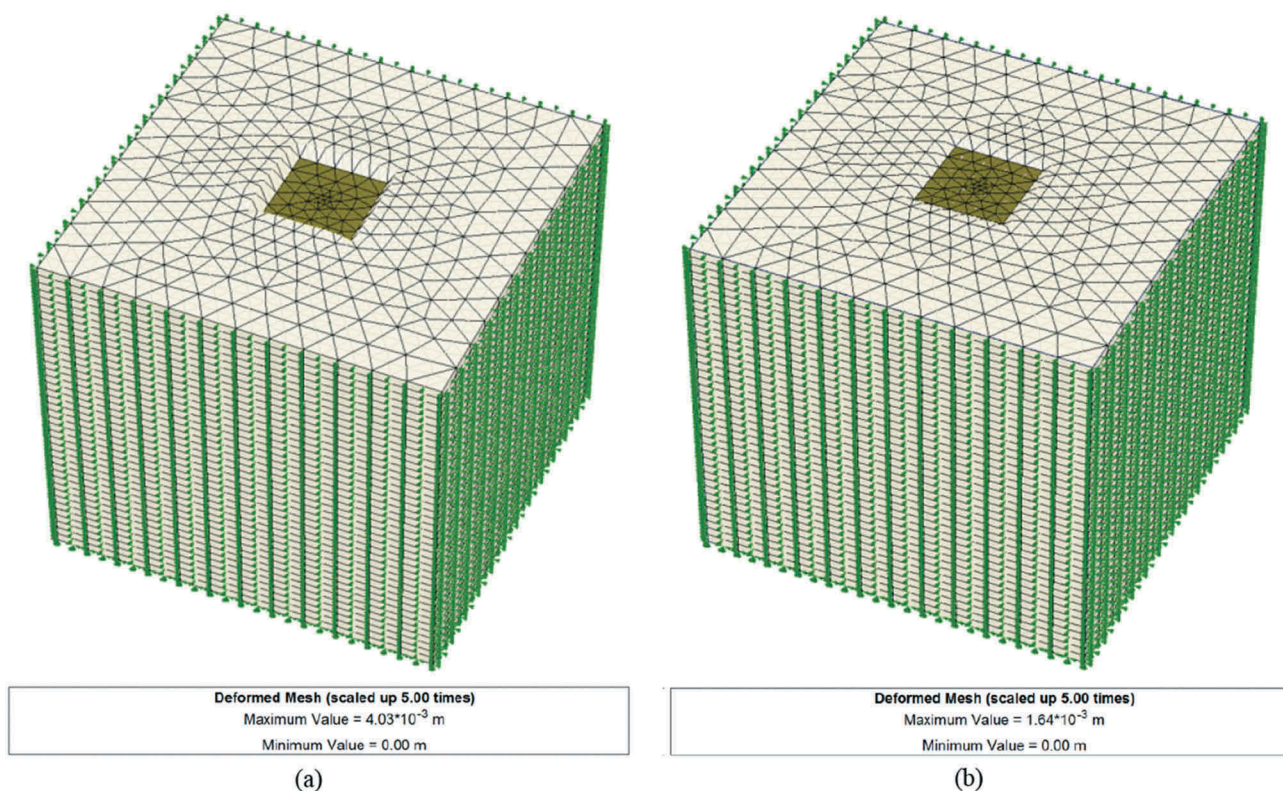


Figure 2. (a). Deformed mesh of raft and (b) piled raft with soil domain.

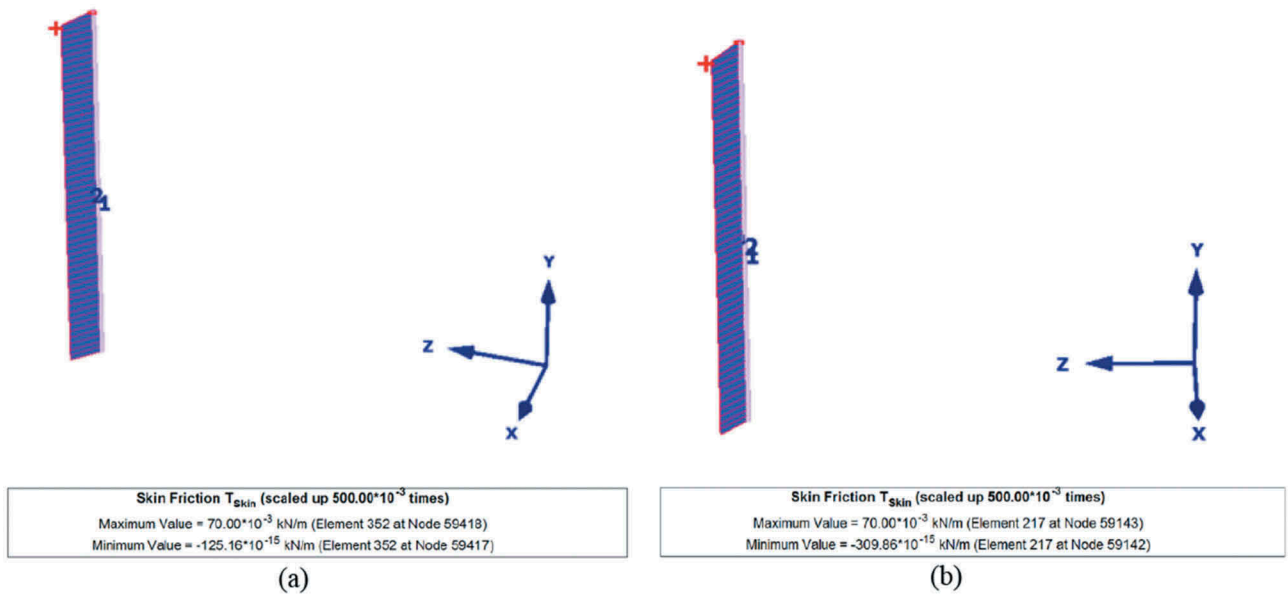


Figure 3. Skin friction mobilisation for the (a) corner pile and (b) centre pile.

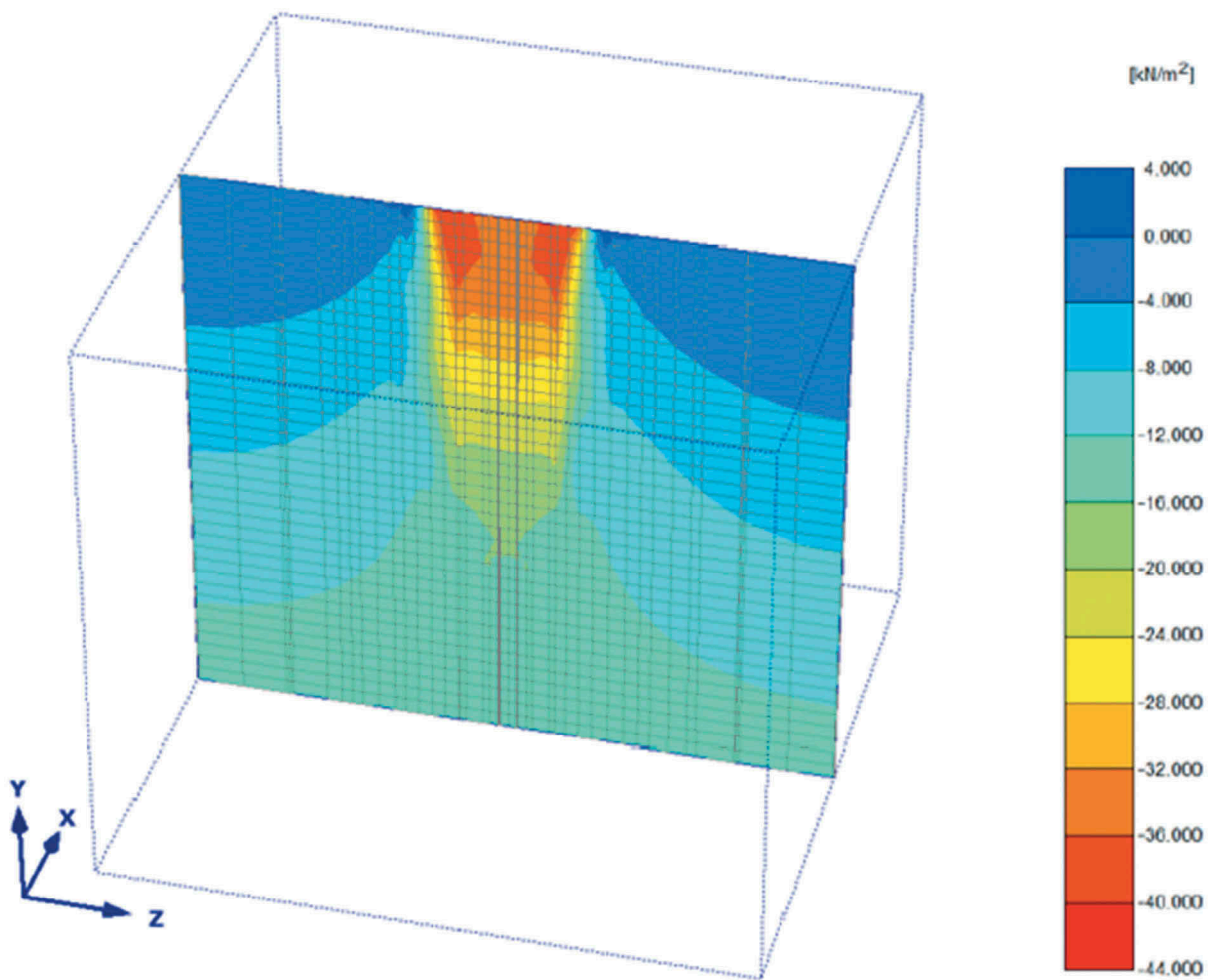


Figure 4. Vertical stress contours at a section taken along the y-axis.

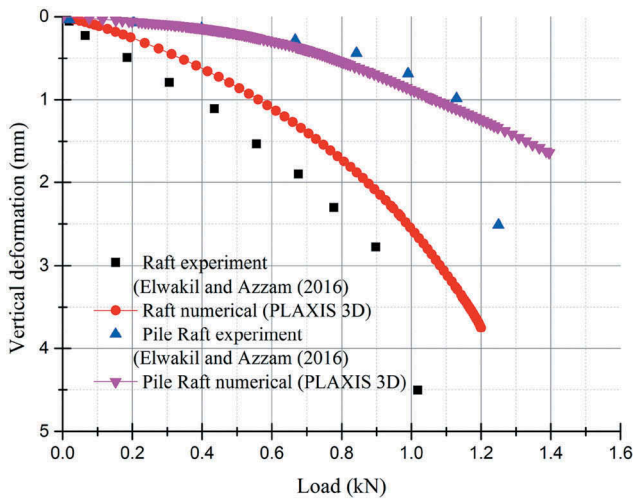


Figure 5. Experiment and numerical simulation of load–deflection curve for a raft and a piled raft.

Table 2. Soil properties used in the analysis.

Soil Parameter	Layer 1	Layer 2	Layer 3	Layer 4	Layer 5
Poisson's ratio	0.3	0.35	0.35	0.45	0.45
Young's Modulus (MPa)	24.96	35.01	29.97	80.01	90
Angle of friction (ϕ) (Degree)	30	35	5	0	0
Cohesion (c') (kPa)	3	5	25	55	70
Unit Weight (kN/m^3)	20	20	17	21	21
Layer thickness (m)	6	6	13	10	35

the static loading (for the case of 15 m pile length with 5 m c/c spacing). From the vertical displacement contours, it may be seen that the pressure bulb has completely formed

without any artificial boundary effects. Also, the soil deformation reduces gradually in the horizontal direction away from the piled raft. From the stress contours, it may be observed that the vertical stresses are free field (or in-situ) in nature away from the piled raft in both vertical and lateral directions. These indicate that the chosen soil dimension is sufficiently large to be free from any boundary effect. The side vertical boundaries of the soil domain are assumed to be on rollers, that is, the vertical movements are only allowed at these boundaries. The bottom of the soil is assumed to be fixed, that is, both the horizontal and the vertical movements are restricted. In this case, as the piled raft is resting on a multilayered soil, the skin friction has been taken to be layer dependant with the value of $R_{inter} = 0.67$ for all the layers. The plasticity properties of the skin friction are derived from the adjacent soil properties. The maximum skin resistance and the base resistance of the embedded pile are 40kN/m and 70kN for all the cases. The stress change in the soil during a pile installation is not included (wished in place) in modelling the bored piles. The piles are assumed to be in a stress-free state at the start of the numerical analysis as assumed by Jeong *et al.* (2004).

3.1. Numerical study

A series of numerical analyses on the piled raft (PR) is performed with different pile lengths, pile spacing and configurations with varying pile group to raft area ratio (B_g/B_r), as shown in Figures 8 and 9, where B_g is the peripheral area of the pile group and B_r is the total area of the raft.

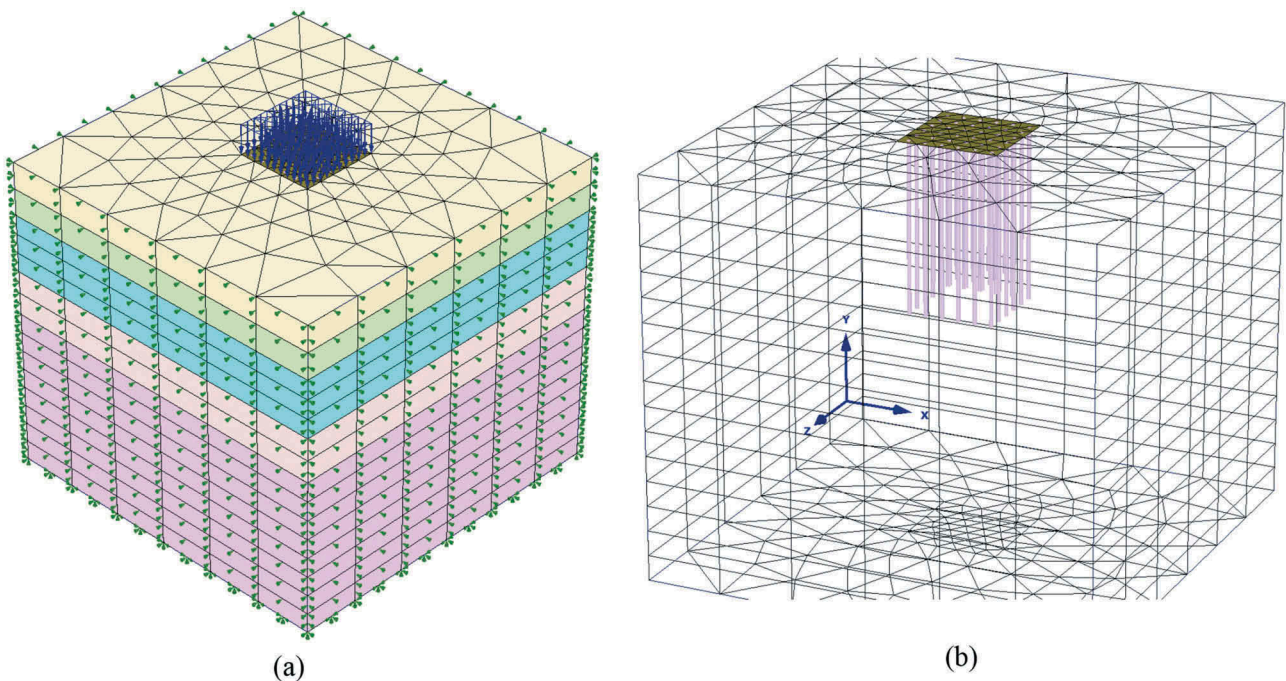


Figure 6. (a) A typical 3D finite element mesh and (b) raft and piles in the mesh (scale factor: 1:40).

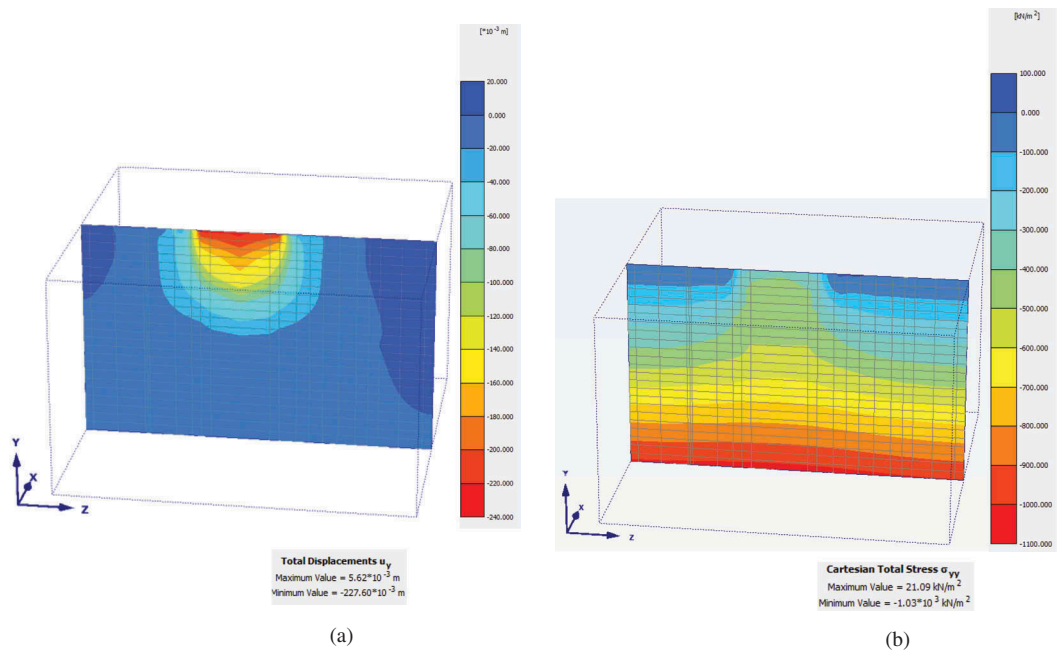


Figure 7. (a) Displacement contours and (b) vertical stresses at a section taken along the y-axis in the piled raft.

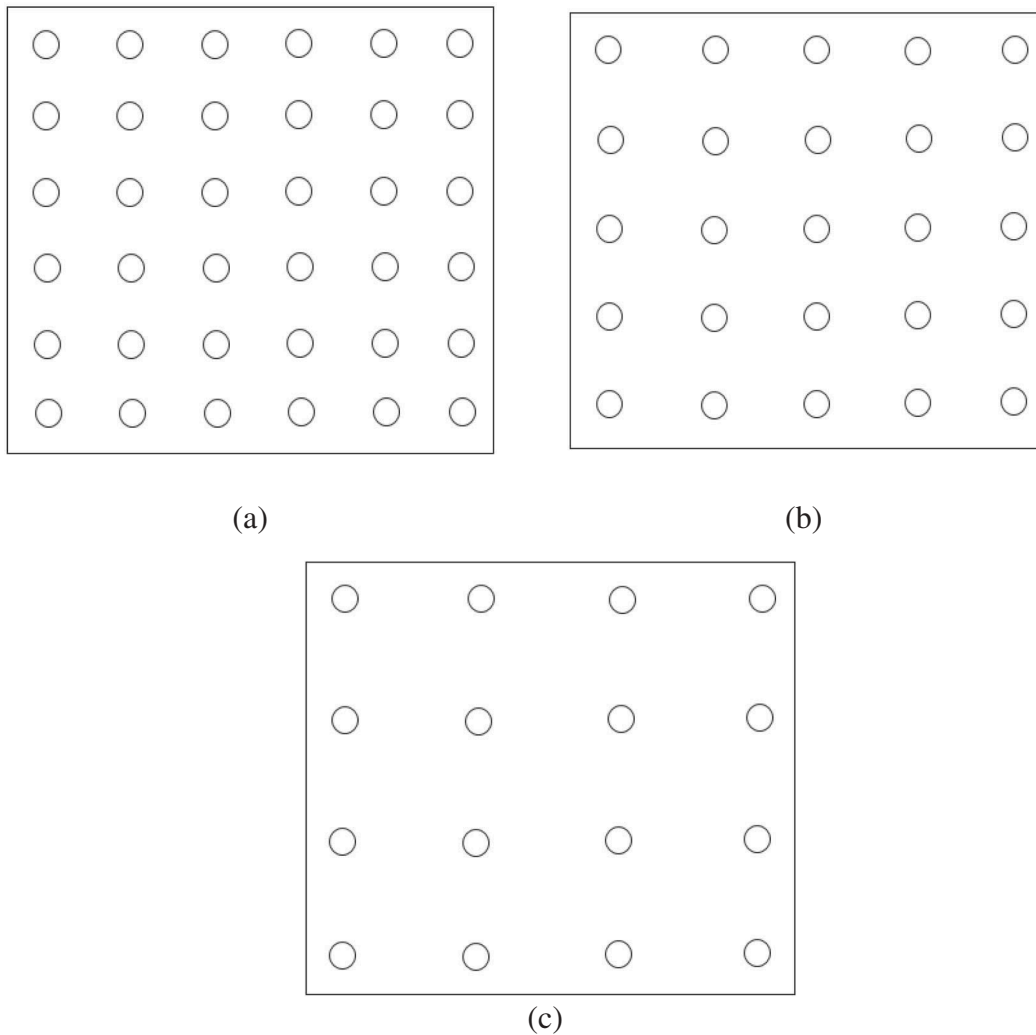


Figure 8. Piled raft with pile spacing of (a) 2.4 m (b) 3.75 m and (c) 5 m c/c.

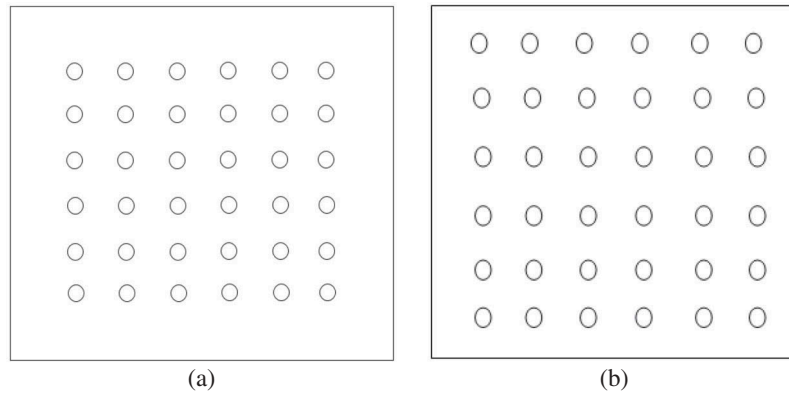


Figure 9. Piled raft with pile group to raft area ratio (B_g/B_r) of (a) 0.47 and (b) 0.84.

The centre to centre pile spacing of 2.4 m, 3.75 m and 5.0 m is considered in the analyses. The vertical settlements at the centre (S_{center}) and at the top right-hand corner (S_{corner}) of the raft are obtained from the 3D finite element analysis and the average settlement, S_{avg} , of the raft is computed from the relationship (Reul and Randolph 2004):

$$S_{avg} = \frac{(2S_{center} + S_{corner})}{3} \quad (6)$$

where S_{avg} is the average settlement of the raft. S_{center} is the settlement at the centre. S_{corner} is the settlement at the right-hand corner of the raft.

The differential settlement of the raft is computed as $S_{c-c} = S_{center} - S_{corner}$, which represents the settlement of the centre of the raft with respect to its top right-hand corner (Cho *et al.* (2012)). The ultimate bearing capacity

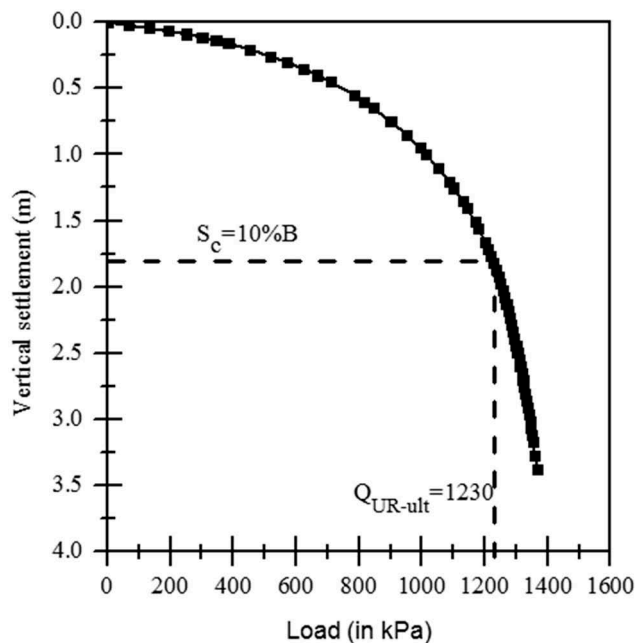


Figure 10. The load-settlement curve of an un-piled (UR) raft.

of the raft without piles (Q_{UR-ult}) is estimated from the load–settlement relationship for the raft for a load corresponding to a settlement of 10% of the width (B) of the raft (Cooke (1986), de Sanctis and Mandolini (2003), de Sanctis and Mandolini (2006)). Figure 10 shows the pressure (P)–settlement (S) curve for the raft without any pile. From this figure, the value of Q_{UR-ult} is found to be 1230 kPa.

3.2. Effect of pile spacing on a piled raft

To study the effect of pile spacing on the behaviour of a piled raft, the normalised vertical load (P/Q_{UR-ult}) and the corresponding average settlement ratio (S_{avg}/B) of a raft alone and a piled raft with 2.4 m, 3.75 m and 5.0 m c/c pile spacing are shown in Figure 11. The pile length for all the

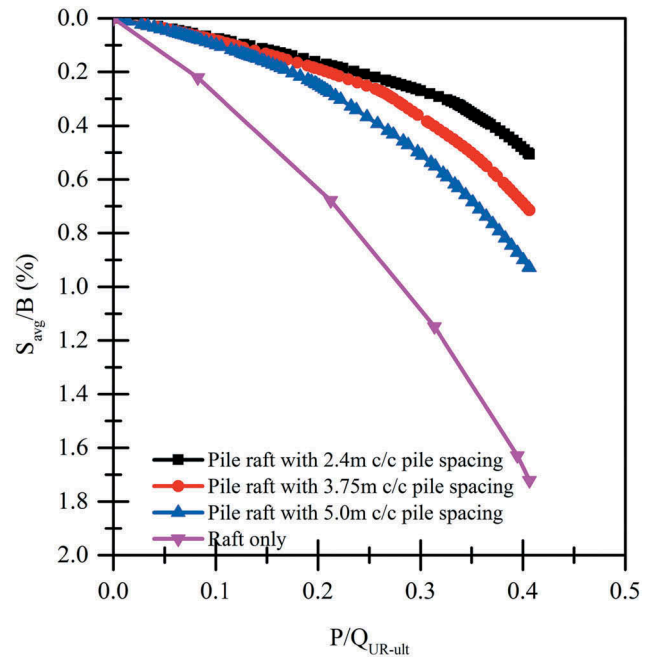


Figure 11. Normalised load vs. average settlement of piled rafts with different pile spacings.

Table 3. Settlements corresponding to various pile configurations.

Pile Configuration	Settlement (mm) corresponding to 200 kPa vertical load
Raft only (UPR)	90
Pile raft with 3D pile spacing	23
Pile raft with 4D pile spacing	26
Pile raft with 5D pile spacing	33

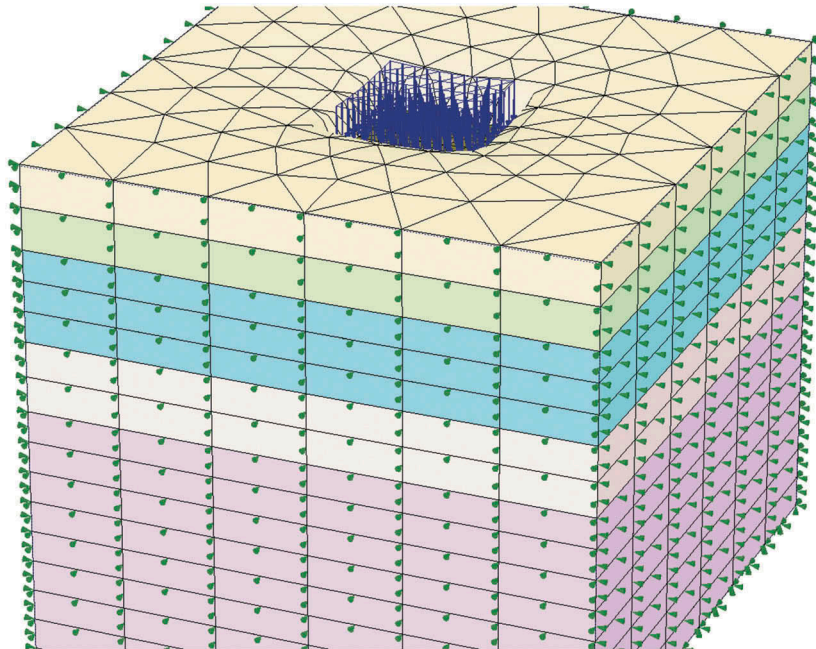
cases is kept constant at 25 m. The load–settlement curve shows an increasing trend as the normalised vertical load increases, but for a particular value of load, the settlement value decreases as the spacing between the piles decreases. The settlement of the raft corresponding to a representative vertical load of 200 kPa ($P/Q_{UR-ult} = 0.16$) for different pile spacings is shown in Table 3. The deformed mesh and the vertical deformation contours corresponding to a vertical load of 500 kPa in a piled raft with 5D pile spacing are shown in Figures 12 and 13. The differential settlement of the piled raft (S_{c-c}) along with the applied loading (P) is shown in Figure 14 for 3D, 4D and 5D pile spacing underneath the raft. In all the cases, the length of the piles is assumed to be 25 m. For the comparison purpose, the differential settlement of the un-piled raft is also shown in the same figure. It may be observed from the above figure that the differential settlement of the raft gradually reduces with the decrease in the pile spacing, as expected, and the overall behaviour of the piled raft improves. The effect of pile spacing, in terms of inverse of pile spacing, $1/S$ (m^{-1}), on the differential displacement, S_{c-c} is shown in Figure 15 for two P/Q_{UR-ult} ratios of 0.167 and 0.406. It may be observed that the differential settlement is less for lesser load (P/Q_{UR-ult}). Also, beyond certain pile spacing, the

differential settlement curve becomes flat for P/Q_{UR-ult} of 0.167 which is not observed for P/Q_{UR-ult} of 0.406. The number of piles underneath the raft corresponding to the pile spacing of 2.4, 3.75 and 5 m c/c is 36, 25 and 16, respectively. Hence, the differential settlement for $P/Q_{UR-ult} = 0.167$ is 8 mm (for 16 number of piles), 6 mm (for 25 number of piles) and 4 mm (for 36 number of piles). For $P/Q_{UR-ult} = 0.406$, the differential settlement is 19 mm (for 16 number of piles), 14 mm (for 25 number of piles) and 8 mm (for 36 number of piles). It is observed that as the number of pile increases, the differential settlement reduces.

The axial forces of the centre, side and corner piles in a piled raft with a pile spacing of 3.75 m c/c (locations shown in Figure 16) are studied for two different P/Q_{UR-ult} ratios, 0.167 and 0.406. Figure 17 shows the axial forces in the centre, side and corner piles with depth for the above two load ratios. From Figure 17, it is clearly observed that for a low P/Q_{UR-ult} ratio, the corner pile is subjected to an axial force which is around 1.20 and 1.79 times more than the piles located at the side and the centre of the raft, respectively. But as the P/Q_{UR-ult} ratio becomes high, the individual piles experience higher value of axial loads as compared to those in the previous case. But the side and the corner piles experience the same axial load, which is around 1.11 times more as compared to the pile located at the centre of the raft.

3.3. Effect of pile length in a piled raft

The effect of pile length is shown in Figure 18, in which the load (P) with the average settlement (S_{avg}) of a piled raft is shown for a pile length of 15 m and 25 m with the

**Figure 12.** Deformed mesh for a piled raft with spacing of 5D (scale 1:20).

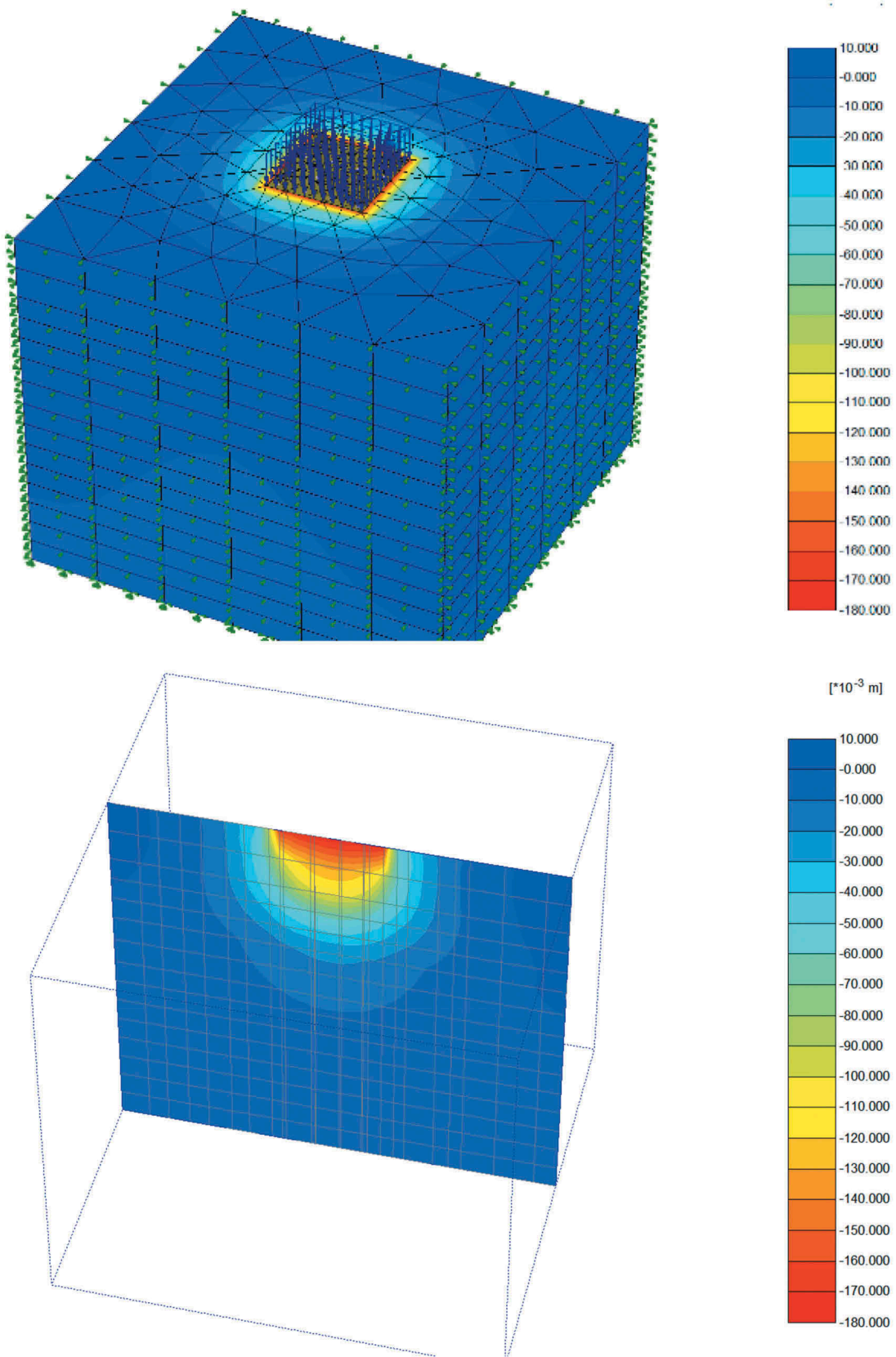


Figure 13. Vertical deformation contours for piled raft with spacing of 5D (Deformation in mm).

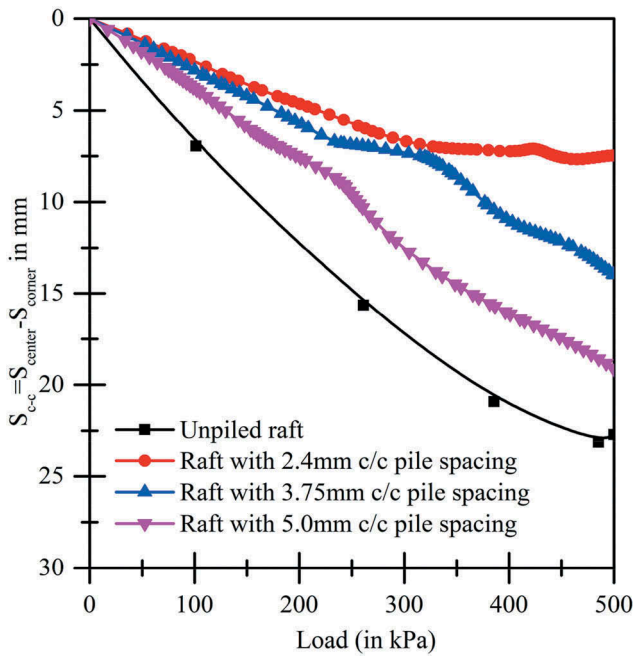


Figure 14. Differential settlements in un-piled and piled raft for different pile spacings.

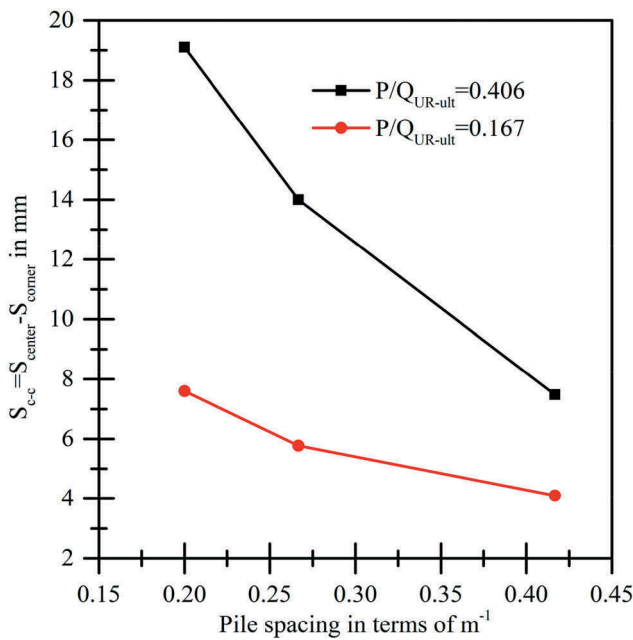


Figure 15. Differential settlement versus pile spacing.

pile spacing of 2.4 m, 3.75 m and 5 m c/c. For a given pile spacing, the settlement of a raft is observed to increase with the decrease in the pile length. To find out an optimum pile length to improve the performance of a piled raft, two configurations of piled raft are considered. In the two pile configurations, combinations of 25 m and 15 m pile lengths are used with their positions fixed strategically to reduce the raft settlement.

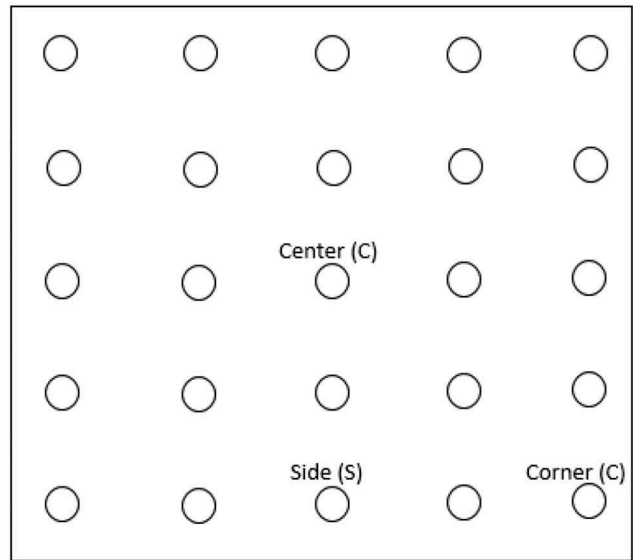


Figure 16. Pile locations at corner, centre and sides in a piled raft.

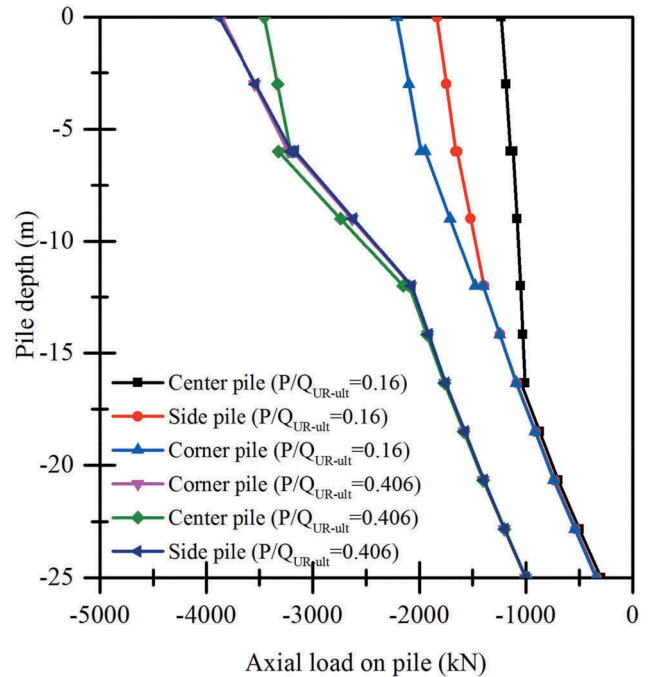


Figure 17. Axial forces on pile with different P/Q_{UR-ult} ratio for a pile spacing of 3D.

In the first configuration, the perimeter piles are 15 m and the inner piles are 25 m in length. The diameter of each pile is assumed to be 0.8 m. In another configuration, the perimeter piles are 30 m in length and the inner piles are 25 m in length. The load average settlement curves are shown in Figure 19 for the above two pile configurations along with a standard case, where all the piles have a length of 25 m. It is observed from Figure 19 that there is a significant improvement in the behaviour

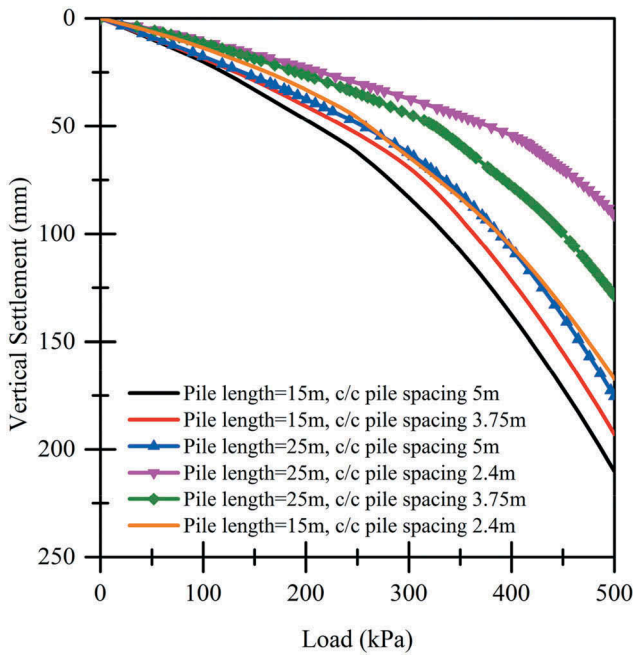


Figure 18. Load-settlement curve for piled rafts with 15 m and 25 m pile length.

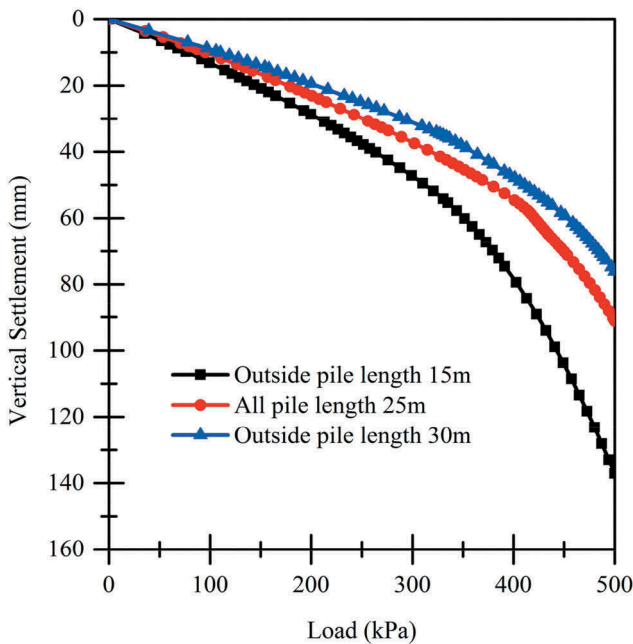


Figure 19. Load-settlement curves for a piled raft with different pile configurations.

of a piled raft if all the outer piles are 30 m in length. As expected, the differential settlement of the raft increases as the pile length is reduced from 25 m to 15 m. For illustration purpose, the differential settlement (S_{c-c}) of a piled raft along with the applied vertical load (P) is shown in Figure 20 for two pile lengths with 3D pile spacing.

Another way of reducing the settlement of a piled raft is by increasing the area of the pile group (B_g) to raft (B_r) ratio. In Figure 21, a typical load average settlement curve for B_g/B_r ratios of 0.47, 0.56 and 0.84 is shown for a pile length of 25 m and a pile diameter of 0.8 m. It is found that as the area of pile group increases from 0.47 to 0.84, there is a drastic reduction in settlement by 2.56 times. The decrease is more pronounced as B_g approaches B_r , hence it is always beneficial to spread the piles uniformly along the entire area of the raft to reduce the overall average settlement. A typical differential settlement between the raft's centre and the edge (S_{c-c}) with the B_g/B_r ratio is shown in Figure 22. As observed from the figure, the differential settlement of the raft decreases, levels off, and then increases as the B_g/B_r ratio increases. The differential settlement is minimum when the B_g/B_r ratio is between 0.4 and 0.6 for most piled rafts, as also reported by Randolph (1994), and Horikoshi and Randolph (1998). This trend holds good for different soil profiles and loading conditions.

3.4. Conclusions

The settlement aspects for an efficient design of a piled raft subjected to vertical loadings in a layered soil have been addressed for different pile spacing, lengths, positions and configurations. As the pile spacing increases, the settlement corresponding to a particular load increases as shown in Table 3. For a given diameter,

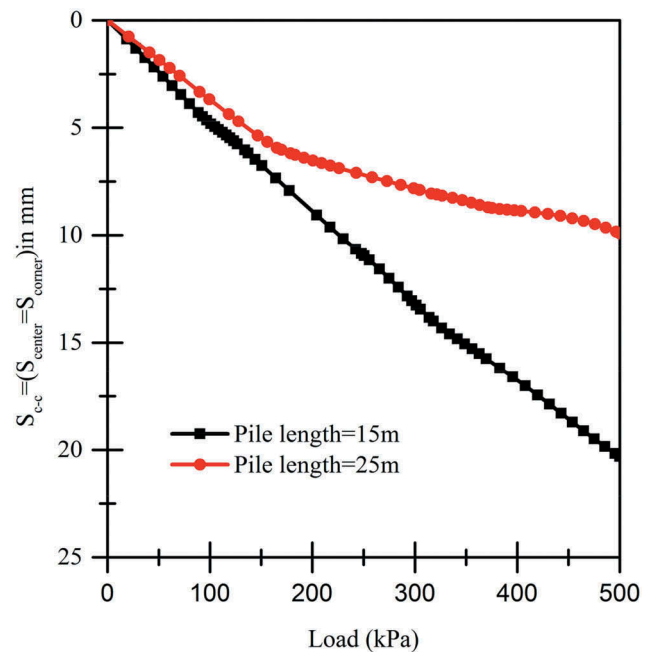


Figure 20. Differential settlement in a piled raft for pile lengths of 15 and 25 m and for a pile spacing of 3D.

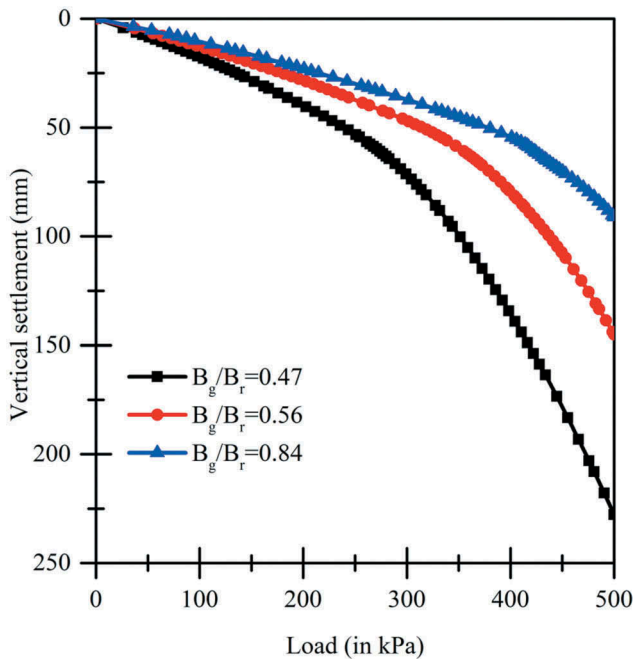


Figure 21. Load–settlement curves for different B_g/B_r ratios.

with the increase in pile length, the average settlement decreases which may be observed from Figure 18. A study has been conducted for different pile group-raft area ratio (B_g/B_r), from which it is concluded that for an efficient design of a piled raft in a layered soil with respect to its serviceability, that is, the differential settlement, the required pile group-raft area ratio (B_g/B_r) in a layered soil should be within a range of 0.4 to 0.6.

Disclosure statement

No potential conflict of interest is reported by the authors.

ORCID

Raj Banerjee  <http://orcid.org/0000-0002-0359-5738>

References

- Balakumar, V., et al., 2013. A design method for piled raft foundations. *Proceedings of the 18th International Conference on Soil Mechanics and Geotechnical Engineering*. Paris, 2671–2674.
- Bourgeois, E., de Buhan, P., and Hassen, G., 2012. Settlement analysis of piled raft foundations by means of a multiphase model accounting for soil-pile interactions. *Computers and Geotechnics*, 46, 26–38. doi:10.1016/j.compgeo.2012.05.015
- Brinkgreve, R.B.J. and Swolfs, W.M., 2007. *PLAXIS 3D foundation. Finite element code for soil and rock analysis*. Netherlands: Users Manual.

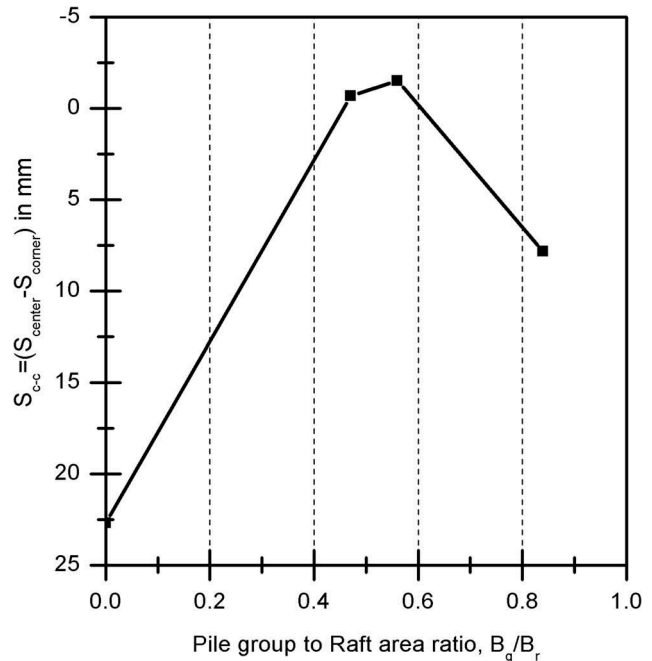


Figure 22. Differential settlement with B_g/B_r ratios.

- Broms, B., 1964a. Lateral resistance of piles in cohesionless soils. *Journal of the Soil Mechanics and Foundations Division, ASCE*, 89 (3), 123–157.
- Broms, B., 1964b. The lateral resistance of piles in cohesive soils. *Journal of the Soil Mechanics and Foundations Division, ASCE*, 90 (2), 27–63.
- Butterfield, R. and Banerjee, P.K., 1971. The problem of pile group and pile cap interaction. *Geotechnique*, 21 (2), 135–142.
- Cho, J., et al., 2012. The settlement behavior of piled raft in clay soils. *Ocean Engineering*, 53, 153–163. doi:10.1016/j.oceaneng.2012.06.003
- Clancy, P. and Randolph, M.F., 1993. An approximate analysis procedure for piled raft foundations. *International Journal for Numerical and Analytical Methods in Geomechanics*, 17 (12), 849–869.
- Cooke, R.W., 1986. Piled raft foundations on stiff clays: a contribution to design philosophy. *Geotechnique*, 36 (2), 169–203. doi:10.1680/geot.1986.36.2.169.
- de Sanctis, L. and Mandolini, A., 2003. On the ultimate vertical load of piled rafts on the soft clay soils. *Proceedings of 4th international geotechnical seminar on deep foundation on bored and auger piles*. Ghent: Mill press, 379–386.
- de Sanctis, L. and Mandolini, A., 2006. Bearing capacity of piled rafts on soft clay soils. *Journal of Geotechnical & Geoenvironmental Engineering (ASCE)*, 132 (12), 1600–1610. doi:10.1061/(ASCE)1090-0241(2006)132:12(1600).
- EI-Garhy, B., et al., 2013. Behavior of raft on settlement reducing piles: experimental model study. *Journal of Rock Mechanics and Geotechnical Engineering*, 5 (5), 389–399. doi:10.1016/j.jrmge.2013.07.005.
- Elwakil, A.Z. and Azzam, W.R., 2016. Experimental and numerical study of piled raft system. *Alexandria Engineering Journal*, 55 (1), 547–560. doi:10.1016/j.aej.2015.10.001.

- Engin, H.K., 2006. A report on embedded piles. Plaxis internal report.
- Franke, E., 1991. Measurements beneath piled rafts. Keynote lecture to ENPC Conference on Deep Foundation. Paris.
- Franke, E., Lutz, B., and El-Mossallamy, Y., 1994. Measurements and numerical modelling of high-rise building foundations on frankfurt clay. *Geot Spec Pub*, 40 (2), 1325–1336.
- Horikoshi, K. and Randolph, M.F., 1998. A contribution to the optimum design of piled rafts. *Geotechnique*, 48 (2), 301–317. doi:10.1680/geot.1998.48.3.301.
- Ibrahim, A.M., 2013. Pile raft foundation with piles act as settlement reducer. *Resources and geotechnical engineering*, Vol. 10. Freiberg: Institut für Geotechnik Gustav-Zeuner-Straße, 1, 09596.
- Jeong, S., et al., 2004. Time dependant behavior of pile groups by staged construction of an adjacent embankment on soft clay. *Canadian Geotechnical Journal*, 41, 644–656.
- Katzenbach, R., et al., 2005. Combined pile raft foundations (CPRF): an appropriate solution for the foundations of high-rise buildings. *Slovak Journal of Civil Engineering*, 3, 19–29.
- Lee, S.W., et al., 2010. Modelling of piled rafts with different pile models. *Proceedings of the 7th European Conference on Numerical Methods in Geotechnical Engineering*. Trondheim, Norway: CRC Press, 637–642.
- Matlock, H., 1970. Correlations for design of laterally loaded piles in soft clay. *2nd Annual Offshore Tech. Conf.*, Vol. 1. Houston, Texas, 577–588.
- Matlock, H. and Reese, L.C., 1960. Generalized solutions for laterally loaded piles. *Journal of Soil Mechanics & Foundations Division, ASCE*, 86, 63–91.
- Meyer, B.J. and Reese, L.C., 1979. Analysis of single piles under lateral loading. Report No. FHWA/TX-79/38. Austin, Texas, USA: Texas State Department of Highways and Public Transportation, Transportation Planning Div.
- Nguyen, D.D.C., Jo, S.B., and Kim, D.S., 2013. Design method of piled-raft foundations under vertical load considering interaction effects. *Computers and Geotechnics*, 47, 16–27. doi:10.1016/j.compgeo.2012.06.007
- Park, D., Park, D., and Lee, J., 2016. Analyzing load response and load sharing behavior of piled rafts installed with driven piles in sands. *Computers and Geotechnics*, 78, 62–71. doi:10.1016/j.compgeo.2016.05.008
- Poulos, H.G., 1971. Behavior of laterally loaded piles: I- single piles. *Journal of the Soil Mechanics and Foundations Division, ASCE*, 97 (5), 711–731.
- Poulos, H.G., 1994. An approximate numerical analysis of pile-raft interaction. *International Journal for Numerical and Analytical Methods in Geomech*, 18 (2), 73–92.
- Poulos, H.G., 2001. Piled raft foundations: design and applications. *Geotechnique*, 2 (2), 95–113. doi:10.1680/geot.51.2.95.40292.
- Rabiei, M. and Choobbasti, A.J., 2016. Piled raft design strategies for high rise buildings. *Geotechnical Geological Engineering*, 34 (1), 75–85. doi:10.1007/s10706-015-9929-x.
- Randolph, M.F., 1994. Design methods for pile groups and piled rafts. S.O.A. Report, 13 ICSMFE. Vol. 5, 61–82. New Delhi.
- Reese, L.C., 1977. Laterally loaded piles: program documentation. *Journal of the Geotechnical Engineering Division, ASCE*, 103 (4), 287–305.
- Reese, L.C. and Junius, D.A., 1977. *Drilled shaft design and construction manual*. Vol. 2, USA: US Dept. of Transportation, FHA.
- Reul, O. and Randolph, M.F., 2004. Design strategies for piled rafts subjected to nonuniform vertical loading. *Journal of Geotechnical & Geoenvironmental Engineering, ASCE*, 130 (1), 1–13. doi:10.1061/(ASCE)1090-0241(2004)130:1(1).
- Sadek, M. and Shahrour, I., 2004. A three dimensional embedded beam element for reinforced geomaterials. *International Journal of Geomechanics, ASCE*, 4 (2), 931–946.
- Ta, L.D. and Small, J.C., 1996. Analysis of piled raft systems in layered soils. *International Journal for Numerical and Analytical Methods in Geomechanics*, 20 (1), 57–72.